Cellulose (2013) 20:2427–2437
DOI 10.1007/s10570-013-9997-0

ORIGINAL PAPER

Effects of pretreatments on crystalline properties and morphology of cellulose nanocrystals

Dong Yang · Xin-Wen Peng · Lin-Xin Zhong · Xue-Fei Cao · Wei Chen · Run-Cang Sun

Received: 20 March 2013 / Accepted: 8 July 2013 / Published online: 3 August 2013

Abstract Cellulose nanocrystals (CNCs) have drawn tremendous attention because of their extraordinary physical and chemical properties as well as renewability and sustainability. In this work, after a range of pretreatments, such as freeze-drying, ball-milling, mercerization, *N*-methylmorpholine-*N*-oxide dissolution and ionic liquid dissolution, various CNCs with different crystalline properties and morphologies were obtained by hydrolysis or oxidation. XRD and AFM were used to determine the influences of pretreatments on the crystalline properties and morphologies of CNCs. New methods, i.e., specific pretreatments followed by sulfuric acid hydrolysis or 2,2,6,6-tetramethylpiperidine-1-oxyl radical (TEMPO) oxidation, were developed to obtain sphere-like CNCs. It was found that sphere-like CNCs were more likely to be obtained from cellulose materials possessing high accessibility. Pretreatments produced cellulose with various crystallinities and polymorphs, and therefore changed the yields of CNCs and influenced their morphology. CNCs prepared by TEMPO oxidation generally had smaller size than the corresponding products obtained by sulfuric acid hydrolysis. In addition, for the dissolved/regenerated cellulose, TEMPO oxidation was a better method to yield sphere-like CNCs than sulfuric acid hydrolysis.

Keywords Cellulose nanocrystals · Pretreatments · Sulfuric acid hydrolysis · TEMPO-assisted oxidation

D. Yang · X.-W. Peng · L.-X. Zhong (✉) · X.-F. Cao · W. Chen · R.-C. Sun (✉)
State Key Laboratory of Pulp and Paper Engineering, South China University of Technology, Guangzhou, China
e-mail: lxzhong0611@163.com

R.-C. Sun
e-mail: rcsun@scut.edu.cn; ynsun@scut.edu.cn; rcsun3@bjfu.edu.cn

L.-X. Zhong · R.-C. Sun
Beijing Key Laboratory of Lignocellulosic Chemistry, Beijing Forestry University, Beijing 100083, China

Introduction

Cellulose nanocrystals (CNCs) are attractive renewable materials by virtue of their biocompatibility, excellent mechanical strength, unique self-assembly and high surface activity (Habibi et al. 2010; Klemm et al. 2011). Thus, a wide range of CNC applications have been developed in recent years, such as composite films, hydrogels, coatings, pharmaceuticals and food packaging (Aulin et al. 2009; Azizi Samir et al. 2004; Goetz et al. 2009). Typically, CNCs are prepared by removing amorphous areas of cellulose materials by means of mineral acid hydrolysis. The morphology and particle size of CNCs are strongly dependent on the hydrolysis condition and cellulose sources (Bondeson et al. 2006; Klemm et al. 2011).

Generally, CNCs are rod-like. For example, Beck-Candanedo et al. (2005) reported that after 64 wt% sulfuric acid hydrolysis, rod-like CNCs with a length of 147 ± 7 nm were obtained from eucalyptus pulp. Van den Berg et al. (2007) successfully produced rod-like tunicate cellulose whiskers with a width of 20 nm and length of 1–2 mm by means of HCl hydrolysis (3 M) under ultrasonic treatment. However, NaOH and DMSO pre-swelling in a combination of H_2SO_4/HCl hydrolysis could produce sphere-like CNCs with particle sizes ranging from 60 to 570 nm (Zhang et al. 2007). Wang et al. (2007a) obtained spherical 20–90-nm-diameter CNCs by mixed acid (H_2SO_4 and HCl) hydrolysis under ultrasonic treatment.

The properties of CNC, such as size, shape, surface charge, etc., are closely related to their performances and applications in specific fields. In theory, CNCs with a higher aspect ratio (length/width) will make a greater contribution to the mechanical strength of composites, but are harder to disperse and more likely to become entangled in suspension (Habibi et al. 2010). On the other hand, for composites, shorter CNCs could increase the crystallinity of the matrix (Siqueira et al. 2008). The CNC surface charge has significant impacts on their performances as well. CNCs with sulfate groups exhibit poor thermal stability, but high dispersibility in aqueous solution (Araki et al. 2000). Moreover, CNC morphology is a key factor influencing the phase separation and formation of chiral nematic suspensions. Sphere-like CNCs are more inclined to form crystallization colloids rather than the liquid crystalline phase above the critical concentration (Elazzouzi-Hafraoui et al. 2007).

Given the need to obtain CNCs with a certain shape, the influencing factors, such as the type of mineral acid, acid concentration, hydrolysis temperature, reaction time and cellulose sources, have been discussed and listed in several reviews (Terech et al. 1999; Bondeson et al. 2006). In addition, pretreatments and different hydrolysis systems were used to obtain CNCs with different properties. Isogai et al. (2008, 2009) investigated the effect of several pretreatments on the degree of CNC polymerization obtained by 2,2,6,6-tetramethylpiperidine-1-oxyl radical (TEMPO)-assisted oxidation and also confirmed that dissolution/regeneration pretreatment decreased the leveling-off degree of polymerization of cellulose in sulfuric acid hydrolysis. However, an important work, which reveals the relations between pretreatment and characteristics of CNC, has not been reported yet.

In this study, freeze-drying, ball-milling, mercerization, *N*-methylmorpholine-*N*-oxide (NMMO) dissolution and BmimCl dissolution, processes that have been extensively applied in cellulose research, were used as pretreatments for CNC preparation, followed by sulfuric acid hydrolysis or TEMPO-assisted oxidation. An atomic force microscope was used to determine the morphology and particle size of the obtained CNCs, and the crystalline structure was detected by X-ray diffraction. In this work, several new methods were explored for yielding sphere-like CNCs. Further, the relations between different pretreatments and the yield, morphology and crystallinity properties of the corresponding CNCs obtained were thoroughly studied and discussed.

Materials

Cotton linter with a particle size of 200 mesh was purchased from Xuanyuan Machinery, Shandong, China. The α-cellulose content was over 98 wt%, and the ash was <0.1 wt%. The viscosity average degree of polymerization of linters measured in CUEN solution was 780 glucose units on average. TEMPO, sodium bromide (NaBr) and 7 % sodium hypochlorite (NaClO) solution were laboratory grade and purchased from Sigma-Aldrich Co., Ltd., China. BmimCl (≥99 %) was purchased from Chengjie Chemistry Co., Ltd., Shanghai, China. NMMO containing 50 wt% water was purchased from Aladdin Chemistry Co., Ltd., Shanghai, China. Analytical grade sulfuric acid (H_2SO_4) and sodium hydroxide (NaOH) were purchased from Guanghua Sci-Tech Co., Ltd., Guangdong, China.

Methods

In order to prepare CNCs, a two-step process, i.e., pretreatment and subsequent hydrolysis or oxidation, was used in this work, as shown in Fig. 1. In the first step, cotton linter was pretreated by different methods, such as ball-milling, mercerization, dissolution, etc. In the second step, the pretreated cotton linter was hydrolyzed into CNCs by H_2SO_4 hydrolysis or TEMPO-assisted oxidation. The specific conditions

of pretreatment and/or oxidation are described below in detail, and the abbreviations are listed in Table 1.

Mechanical pretreatment

Linter was ball-milled for 24 h with a frequency of 1,000 rpm to prepare ball-milled cellulose (marked as BM-n). In order to obtain freeze-dried materials (marked as FD-n), linter was soaked in deionized water of tenfold weight with agitation for 1 h and then freeze-dried and stored in a dryer.

Mercerization

Cotton linter was soaked in 20 wt% NaOH aqueous solution with a solid-to-liquid ratio of 1:8 (g/ml) at 30 °C for 2 h with 400 rpm stirring. The pretreated cellulose was washed thoroughly with water, dried in an oven and stored in a dryer (marked as SH-n).

NMMO pretreatment

The 50 wt% NMMO/H_2O mixture was dehydrated in a solution containing 90 wt% NMMO by a vacuum rotatory evaporator. Then linters were suspended in the concentrated NMMO solution with a solid content of 10 % (g/ml) at 80 °C for 30 min and proved to be dissolved by polarized microscope. The dissolved cellulose was regenerated by excess water, thoroughly washed with water and then dried in an oven (marked as NM-n).

Ionic liquid pretreatment

Cotton linter was added to BmimCl with a concentration of 2 wt%. The dissolution was carried out at 105 °C for 6 h with 300-rpm stirring. Then excess ethanol was gradually dropped into the solution as an anti-solvent (marked as IL-n). The dissolved/regenerated (D/regenerated) cellulose was thoroughly washed with water and dried in an oven.

Sulfuric acid hydrolyzation

Cellulose was suspended in 64 wt% H_2SO_4 with a solid-to-liquid ratio of 1:10 (g/ml) and reacted at 40 °C for 2 h (marked as S2) or 4 h (marked as S4), with stirring at 600 rpm. Upon completion of the reaction, the hydrolysis suspension was centrifuged and dialyzed against deionized water for several days. A driblet of purified CNC suspension was extracted, diluted and stored at 4 °C for AFM analysis. The rest of the suspension was freeze-dried, weighed and stored in a desiccator.

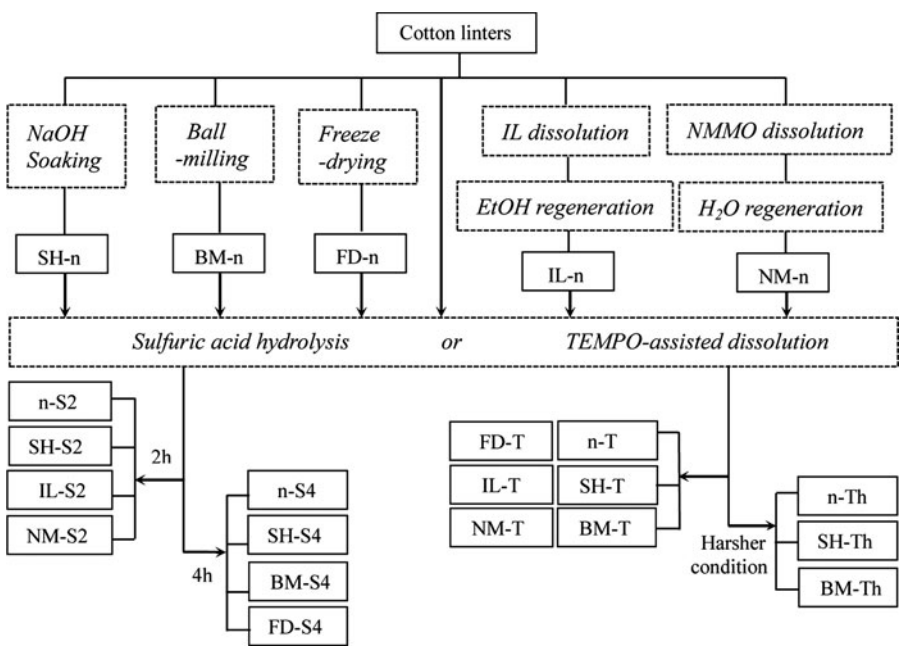

Fig. 1 Experimental scheme of CNC preparation by different methods

Table 1 Yields and crystallinity of CNC prepared by various methods

Pretreatment	Hydrolysis	Code name	Yield (%)	Crystallinity (%)
None	None	n-n	–	57.2
	H_2SO_4, 2 h	n-S2	12.8	72.1
	H_2SO_4, 4 h	n-S4	7.9	73.2
	TEMPO	n-T	45.7	65.3
	TEMPO-h	n-Th	37.2	–
Freeze-drying	None	FD-n	–	54.9
	H_2SO_4, 4 h	FD-S4	12.5	74.1
	TEMPO	FD-T	56.3	52.2
Ball-milling	None	BM-n	–	21.9
	H_2SO_4, 4 h	BM-S4	7.7	68.4
	TEMPO	BM-T	48.5	57.8
	TEMPO-h	BM-Th	15.5	–
Mercerization	None	SH-n	–	46.8
	H_2SO_4, 2 h	SH-S2	7.8	60.3
	H_2SO_4, 4 h	SH-S4	6.3	68.9
	TEMPO	SH-T	36.6	62.3
	TEMPO-h	SH-Th	1.3	–
NMMO regeneration	None	NM-n	–	40.1
	H_2SO_4, 2 h	NM-S2	2.0	29.7
	TEMPO	NM-T	12.9	49.7
BmimCl regeneration	None	IL-n	–	19.7
	H_2SO_4, 2 h	IL-S2	3.5	11.1
	TEMPO	IL-T	9.6	21.5

TEMPO-assisted oxidation

Cellulose (2.0 g) was dispersed in 150 ml water with a homogenizer, and then 0.03 g TEMPO (0.01 mmol/g cellulose) and 0.3 g NaBr (1.46 mmol/g cellulose) were added; 15 ml NaClO solution (20 mmol/g cellulose), which was adjusted to pH = 10.5 by 0.1 M HCl, was mixed into the mixture. The reaction was processed at 30 °C for 4 h with 600 rpm stirring. During oxidation, the pH was maintained at 10.5 by adding 0.5 M NaOH. At the end of the required reaction time, the solution was adjusted to pH = 3.5 by 0.1 M HCl to terminate the reaction, centrifuged and dialyzed against deionized water. A driblet of purified CNC suspension was extracted, diluted and stored at 4 °C for AFM analysis. The rest of the suspension was freeze-dried, weighed and stored in a desiccator (marked as T). For comparison, another set of TEMPO-assisted oxidation was operated with 30 ml NaClO solution (40 mmol/g cellulose) for 8 h, i.e., a harsher condition (marked as Th).

X-ray diffraction

X-ray diffraction measurements of cellulose and CNC powder were carried out on a Bruker D8 ADVANCE X-ray diffractometer equipped with Ni-filtered Cu $K_{\alpha 1}$ radiation with 0.15418 nm wavelength at room temperature. The scattering angle range was 5°–35°, and scans were collected at 40 kV and 40 mA with a step size of 0.04° every 0.2 s. Crystalline information for cellulose I and II was obtained from previous works to calculate their Miller indices (Nishiyama et al. 2002; Langan et al. 2001). After subtraction of a linear background, the peak fitting was carried out using Gaussian line shapes by Jade 6.0 software. The crystallinity of cellulose was calculated by the method reported by Isogai et al. (2008, 2009) and Wada et al. (2004). The crystallinity values of cellulose I in untreated, freeze-dried and ball-milled cellulose were calculated by the ratio of the separated peak area due to cellulose I to the total area under the curve between $2\theta = 5°$ and 35°. The crystallinity values of cellulose

II in mercerized and D/regenerated samples were determined by the ratio of the separated peak area due to cellulose II to the total area under the curve between $2\theta = 5°$ and 35°. It should be mentioned that for BM-S4, which had discernible peaks of both cellulose I and II, the crystallinity was determined by the ratio of the sum of separated peak area of cellulose I and II to the total area under the curve between $2\theta = 5°$ and 35°.

Atomic force microscope

AFM was performed on Nanoscope III (Veeco Co., Ltd., USA). The samples for observation were prepared by dropping the dilute water suspension with about 50 ppm CNC onto a mica surface and then air dried at ambient temperature. All of the images were recorded in tapping mode by silicon cantilevers. Commercial probes were used with a spring constant of 20–80 N/m and a resonance frequency of 300–340 kHz. The scale in all testing was 2.0 μm × 2.0 μm.

Results and discussion

Effect of pretreatments on the crystalline structure of cellulose materials

As shown in Fig. 1, the preparation of CNC involved a physical or chemical pretreatment of cotton linter and the following H_2SO_4 hydrolysis or TEMPO-assisted oxidation. Although the Segal crystallinity index (CI) (Segal et al. 1959) is still used for the determination of cellulose crystallinity because it is readily understood and easily handled, this method does have some shortcomings. For example, French and Santiago Cintrón (2013) demonstrated that comparing CI between different cellulose polymorphs was not accurate. The peak area calculated by curve fitting was confirmed to be more representative than CI for crystalline materials (Driemeier and Calligaris 2011). Therefore, the peak area was selected to characterize cellulose crystallinity in our work.

Figure 2 illustrates the XRD spectra of cellulose materials pretreated by different methods, i.e., the starting materials before hydrolysis or oxidation. Among them, n-n and FD-n showed a typical cellulose I structure, while SH-n and NM-n had a typical cellulose II structure. Besides, the spectra of BM-n and IL-n showed patterns with more amorphous areas. Although not strong, BM-n had a higher intensity at 22.8°, which is related to the 200 plane of cellulose I crystal, and IL-n had a higher intensity at 20.0° corresponding to the cellulose II crystal. Consequently, crystallinity values of starting materials were calculated by the corresponding method and are listed in Table 1. Depending on different crystallinities and crystallite sizes of cellulose materials, variations of $2\theta \pm 0.3°$ were acceptable in positioning the specific peaks.

As shown in Table 1, the crystallinity of FD-n (54.9 %) remained almost the same as that of untreated cellulose n-n (57.2 %), indicating that the swelling and freeze-drying had limited impact on cellulose crystallinity. After ball-milling treatment, the crystallinity decreased to 21.9 %, leading to an increase in cellulose accessibility to reagents (Fan et al. 1981). No noticeable transformation of the cellulose polymorph was observed in the spectrum of BM-n, except for the significant decrease in cellulose I signal. On the other hand, as expected, the cellulose polymorph transformed from crystal I to II for the mercerized and D/regenerated samples. SH-n and NM-n were cellulose II with crystallinities of 46.8 and 40.1 %, which were slightly lower than that of n-n (57.2 %). In mercerization, some factors, such as cellulose sources, temperature and the consistency of the NaOH solution, will affect the crystallinity of mercerized cellulose (Revol et al. 1987; Liu and Hu 2008). Cellulose decrystallization in the NMMO dissolution and regeneration process was also reported

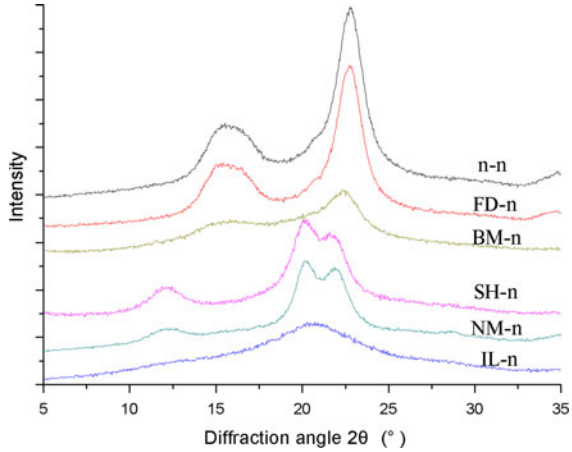

Fig. 2 X-ray diffraction patterns of various pretreated celluloses

by Gao et al. (2011). Moreover, Table 1 shows that IL-n had dramatically decreased crystallinity (19.7 %) after D/regeneration pretreatment. The original crystalline structures of cellulose were destroyed because of the breakage of inter- and intramolecular hydrogen bonds during IL dissolution, and recrystallization in the regeneration process was very limited, resulting in a sharp decrease in crystallinity (Zhang et al. 2005).

Crystalline structure of CNC

The XRD spectra of CNC obtained by sulfuric acid hydrolysis (4 h) are listed in Fig. 3, and their crystallinities and yields are shown in Table 1. FD-S4 had a higher yield (12.5 %) than n-S4 (7.9 %), which must be due to the hornification of cellulose in the freeze-drying process, i.e., a lower accessibility for freeze-dried cellulose (Esteghlalian et al. 2001). The spectrum of BM-S4 was interesting because it showed typical peaks of both cellulose I and II, such as $2\theta = 12.3°$ (-110 plane of cellulose II), 14.8° (-110 plane of cellulose I) and 22.8° (200 plane of cellulose I). Ago et al. (2004) confirmed that the transformation from cellulose crystal I to II could take place with the presence of water in the ball-milling process. The emerging cellulose II was not obvious in the XRD spectrum of BM-n, probably due to its relatively low percentage in BM-n. SH-S4 had a lower crystallinity (68.9 %) and a lower yield (6.3 %) than those of n-S4, illustrating that the CNC prepared from mercerized cellulose had more amorphous areas. The XRD spectra of CNC hydrolyzed by H_2SO_4 for 2 h from mercerized and D/regenerated cellulose are illustrated in Fig. 4. The yields of NM-S2 and IL-S2 were 3.5 and 2.0 %, respectively, which were much lower than those of SH-S2 (7.8 %) and n-S2 (12.8 %), showing good accessibility of D/regenerated cellulose. Meanwhile, the crystallinities of NM-S2 (29.7 %) and IL-S2 (11.1 %) were far less than that of SH-S2 (60.3 %).

As the hydrolytic time was prolonged from 2 to 4 h, the crystallinity of CNC obtained from untreated cellulose increased from 72.1 % (n-S2) to 73.2 % (n-S4), while the yield declined from 12.8 % (n-S2) to 7.9 % (n-S4). Meanwhile, for the mercerized cellulose, the crystallinity increased from 60.3 % (SH-S2) to 68.9 % (SH-S4), whereas the yield decreased slightly from 7.8 % (SH-S2) to 6.3 % (SH-S4). These results illustrated that (1) CNC with higher crystallinity could be obtained by prolonging the hydrolysis time and (2) alkaline treatment assisted in unravelling some rigorous cellulose areas by swelling and therefore reached a relatively stable yield in a shorter time than untreated linters. For TEMPO oxidation, the yield of CNC was also closely related to the reaction condition, as shown in Table 1. When higher concentrations of NaClO (40 mmol/g cellulose) and longer time (8 h) were applied, the CNC (SH-Th) yield was much lower (1.3 %), which is in sharp contrast with SH-T (36.6 %) obtained in milder conditions (20 mmol/g cellulose, 4 h). The yields of n-Th and BM-Th declined to 37.2 and 15.5 %, respectively, when a harsher condition was used. It showed that for well-pretreated cellulose, such as mercerized cellulose, the main hindrances of TEMPO oxidation were

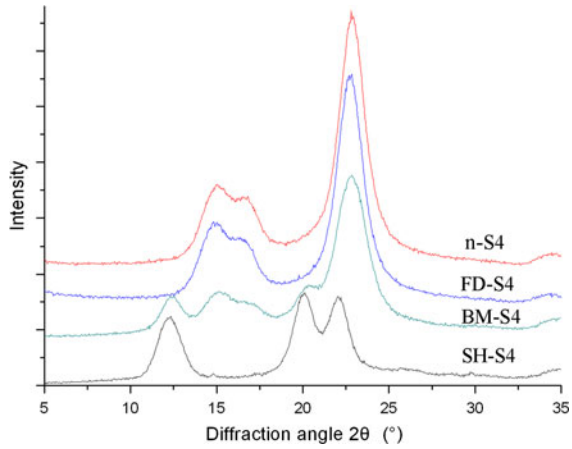

Fig. 3 X-ray diffraction patterns of CNC hydrolyzed by H_2SO_4 for 4 h

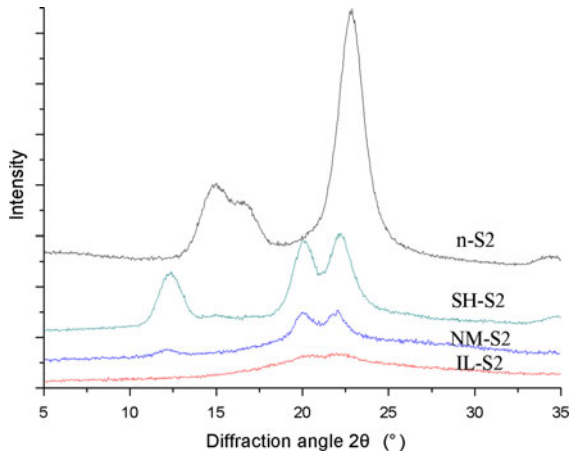

Fig. 4 X-ray diffraction patterns of CNC hydrolyzed by H_2SO_4 for 2 h

the activity of reagents and reaction condition. As compared with previous works (Saito and Isogai 2004), the NaClO dosage was much higher in this work, and therefore the yields of CNC were generally lower. Still, Table 1 illustrates that, in the most cases, CNCs obtained by TEMPO-assisted oxidation had higher yields than those obtained by H_2SO_4 hydrolysis.

In Fig. 5, the XRD spectra of n-T, BM-T and FD-T give patterns of typical cellulose I. After oxidation, the crystallinities of the untreated and freeze-dried cellulose slightly decreased to 65.3 % (n-T) and 52.2 % (FD-T), respectively, whereas the crystallinity of ball-milled cellulose significantly increased from 21.9 % (BM-n) to 57.8 % (BM-T). This phenomenon was accordant with the results of the previous work (Saito and Isogai 2004), in which the crystallinity was nearly unchanged for untreated cotton linter but increased for the low-crystalline cellulose I sample. For mercerized and D/regenerated cellulose, the yield of SH-T (36.6 %) was much higher than those of NM-T and IL-T (12.9 and 9.6 %). Hirota et al. (2010) considered that the main causes were the higher crystallinity and higher degree of polymerization of mercerized cellulose than those of D/regenerated cellulose. Besides, the more accessible macrostructure of NM-T and IL-T may be another cause of the lower yields of NM-T and IL-T. All the crystallinities of TEMPO-oxidized CNC obtained from mercerized and D/regenerated cellulose were found to be higher than those of their corresponding starting materials. From the point of view of yield and crystallinity, TEMPO oxidation was a better method for preparing CNC from D/regenerated cellulose than sulfuric acid hydrolysis.

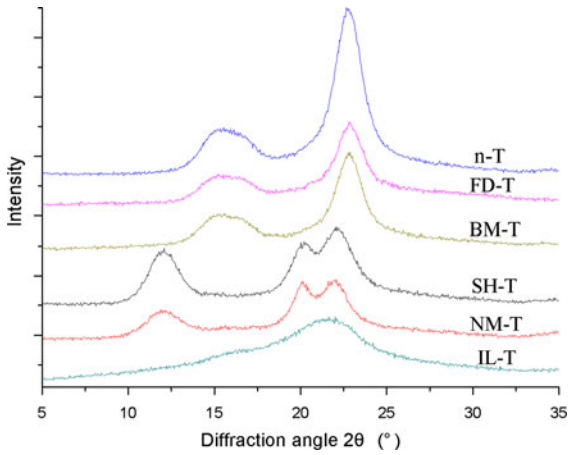

Fig. 5 X-ray diffraction patterns of CNC obtained by TEMPO oxidation

Nanocrystal morphology

AFM was used to study the particle size and morphology of the obtained CNCs, and the results are given in Figs. 6, 7 and 8. Profiles of the lined cross section are shown under the AFM pictures. The dimensions and shapes of the obtained CNCs are listed in Table 2.

Figure 6 shows the features of various CNCs hydrolyzed by H_2SO_4 for 4 h. N-S4s were rod-like particles with a width of 40–60 nm, length of 100–200 nm and height of about 10 nm. These particles agglomerated into bundles after water evaporation for AFM sample preparation. In similar hydrolysis conditions, Elazzouzi-Hafraoui et al. (2007) also produced cotton nanocrystals with a length of 60–200 nm, width of 10–60 nm and average height of around 7 nm. However, after alkali or ball-milling pretreatment, the morphology of CNCs was different from n-S4. Both SH-S4 and BM-S4 tended to form sphere-like particles with a diameter of 100–200 nm and a height of 3–7 nm rather than rod-like particles. Over recent years, analogous spherical CNC has been prepared by HCl/H_2SO_4 mixed acid with ultrasonic assistance or NaOH/DMSO pretreatment (Wang et al. 2007a, b; Zhang et al. 2007). However, in this work, new methods, i.e., various pretreatments in combination with sulfuric acid hydrolysis, were developed to prepare sphere-like CNCs. Generally, acid hydrolysis occurs slowly from the surface to the inner amorphous areas of cellulose, step by step; thus, rod-like CNCs are prepared. Wang et al. (2007a) considered that after suitable pretreatments, e.g., mercerization, the acid molecules were able to penetrate into the inner amorphous areas swiftly. In relatively mild hydrolysis conditions, cellulose material would first be hydrolyzed into micro-level fragments and then gradually into sphere-like CNCs. According to the aforementioned theory, the increased accessibility of SH-n and BM-n contributed to the formation of sphere-like particles. In contrast, FD-S4 had rod-like morphology, which was similar to that of n-S4, perhaps due to the low accessibility of FD-n.

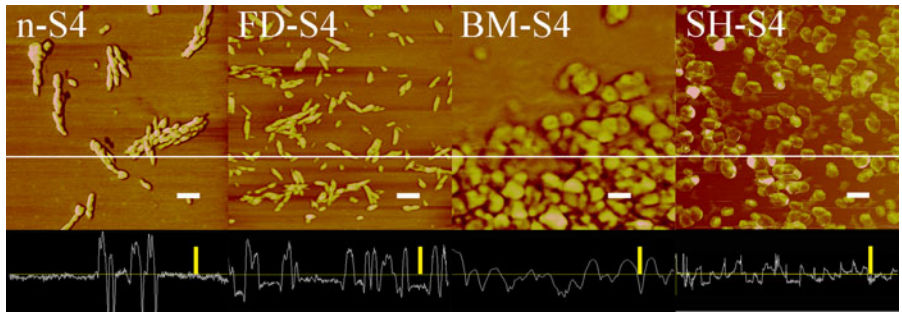

Fig. 6 AFM images and cross-sectional profile of CNC hydrolyzed by H_2SO_4 for 4 h (the length of the *white bars* in AFM images is 200 nm, and the height of the *yellow bars* in the cross-sectional profile is 10 nm). (Color figure online)

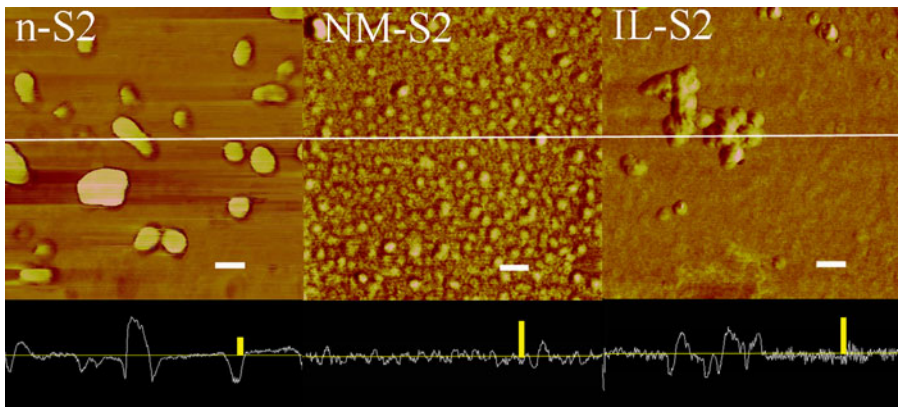

Fig. 7 AFM images and cross-sectional profile of CNCs hydrolyzed by H_2SO_4 for 2 h (the length of the *white bars* in AFM images is 200 nm, and the height of the *yellow bars* in the cross-sectional profile is 10 nm). (Color figure online)

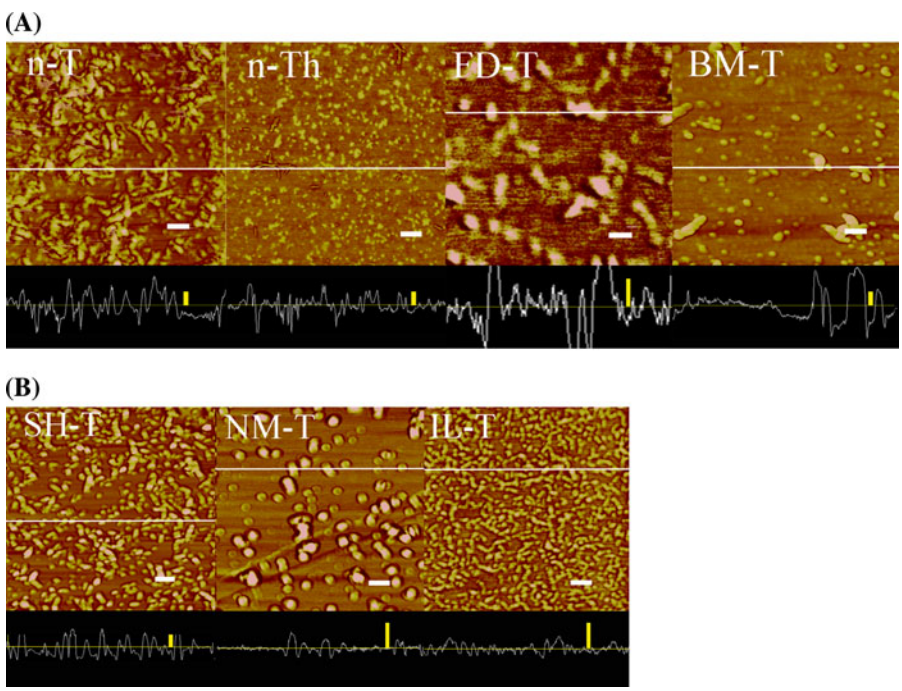

Fig. 8 **a**, **b** AFM images and cross-sectional profile of CNC oxidized by TEMPO (the length of the *white bars* in AFM images is 200 nm, and the height of the *yellow bars* in cross-sectional profile is 10 nm). (Color figure online)

Table 2 Dimensions and shapes of CNCs prepared by various methods

CNC sample	Dimension (nm)	Height (nm)	Morphology
n-S4	100–200 length and 40–60 width	8–15	Rod-like
FD-S4	80–200 length and 30–60 width	8–12	Rod-like
BM-S4	100–200 diameter	3–7	Sphere-like
SH-S4	100–200 diameter	3–7	Sphere-like
n-S2	100–300 diameter	10–20	Irregular and bulky
NM-S2	50–100 diameter	2–5	Sphere-like
IL-S2	50–160 diameter	5–8	Sphere-like
n-T	60–120 length and 30–50 width	10–20	Rod-like
n-Th	30–100 length and 10–30 width for rod-like 20–50 diameter for the granular	8–12	Rod-like or granular
FD-T	100–200 length and 100–150 width	8–20	Irregular and bulky
BM-T	50–100 diameter for sphere-like 100–200 length and 80–150 width for the bulky	10–15	Sphere-like or bulky
SH-T	50–120 diameter	10–15	Sphere-like
NM-T	100–160 diameter	3–8	Sphere-like
IL-T	50–120 diameter	3–7	Sphere-like

CNCs hydrolyzed by H_2SO_4 for 2 h are illustrated in Fig. 7. It was demonstrated that n-S2 consisted of irregular and lumpy particles with a diameter of 100–300 nm and a height of 10–20 nm. As the reaction time increased, the lumps were divided into smaller rod-like particles, as shown in n-S4. NM-S2 and IL-S2 were sphere-like with diameters in the range of 50–120 nm, which were smaller than those of SH-S4. From the cross-sectional profile, NM-S2 demonstrated a much lower height (2–5 nm) than IL-S2 (5–8 nm). NMMO or IL dissolution broke up the original crystalline structure of cellulose, and the recrystallization was limited in anti-solvents, resulting in NM-n and IL-n being more accessible and hydrolyzed into smaller particles.

Figure 8a, b illustrates the AFM images of CNCs prepared by TEMPO oxidation. The reaction condition showed significant impacts on the particle size and shape of the oxidized CNCs. n-Ths, which were oxidized in a higher concentration of NaClO (40 mmol/g cellulose) and for a longer time (8 h), were much smaller compared to n-T oxidized in milder conditions (20 mmol/g cellulose, 4 h). Cellulose bulks in n-T were further oxidized into smaller rods and granules in harsher reaction conditions, which accorded with the previous literature (Habibi et al. 2006).

Also, the pretreatment showed different influences on the morphology of oxidized products. FD-T mainly consisted of bulks with a length of 100–200 nm and a width of 100–150 nm, which was larger than those of n-T. This result showed that the performance of FD-n was different from n-n in TEMPO oxidation, along with distinct yields and crystallinity values of the yielded CNCs. For BM-T, apart from sphere-like particles with diameters of 50–100 nm, some large bulks could be observed because of their incomplete hydrolysis. SH-T and IL-T mainly consisted of sphere-like particles with smilar diameters ranging from 50 to 120 nm, whereas IL-T had a lower height with 3–7 nm than SH-T with 10–15 nm. NM-T was composed of particles with a diameter of 100–160 nm, which were a little larger than those of BM-T, SH-T and IL-T. Interestingly, CNCs oxidized from D/regenerated and mercerized cellulose were sphere-like. The reason may be that the increased accessibility of cellulose to reagent enabled the oxidation to take place on the surface and in the inner amorphous area at the same time. As compared with H_2SO_4 hydrolyzed CNCs, most of the corresponding oxidized CNCs were smaller (except NM-T), which was probably because oxidation could take place on the crystalline surface of cellulose II (Hirota et al. 2010). The size of CNCs was related to the reactive mechanism and was not always

accordant with the yield. Further, besides the higher yield and crystallinity, NM-T and IL-T showed a more homogeneous size distribution than IL-S2 and NM-S2.

According to this study, apart from the influences of hydrolysis and oxidation mechanisms, the accessibility of starting materials was also a determining factor in the particle size and morphology of the obtained CNCs. The crystalline properties and morphology of CNCs could be controlled by altering the crystallinity, cellulose polymorphs and macrostructure of the starting cellulose materials with various pretreatments in this work. Sphere-like CNCs could be easily obtained by sulfuric acid hydrolysis or TEMPO-assisted oxidation when cellulose materials were subjected to mercerization, ball-milling or D/regeneration. The preparation mechanism of CNCs with specific morphologies deserves further study.

Conclusion

In this study, CNCs with different crystalline properties and morphologies were prepared by means of various pretreatments and subsequent sulfuric acid hydrolysis or TEMPO-assisted oxidation. New methods were developed to yield sphere-like CNCs. Dissolution/regeneration pretreatment obviously increased the accessibility of cellulose, while mercerization and ball-milling pretreatments led to a higher accessibility but were not that preferable. The crystallinity, cellulose polymorph and macrostructure of starting materials were the key factors determining the crystalline properties and morphology of CNCs. For the untreated, ball-milled and freeze-dried cellulose, the structure of cellulose was the main hindrance to hydrolysis or oxidation; however, for the mercerized and dissolved/regenerated cellulose, the main hindrances to CNC preparation were the activity of the reagent and the reaction conditions. Sphere-like CNCs could be obtained from cellulose materials with relatively high accessibility, such as ball-milled, mercerized and dissolved/regenerated cellulose. However, these pretreatments led to a low CNC yield, which must be taken into consideration in CNC preparation. For dissolved/regenerated cellulose, TEMPO oxidation was confirmed to be a better method to prepare sphere-like CNCs than sulfuric acid hydrolysis. Along with the further exploration of the relations between the preparation process and properties of CNC, there could be more economical methods for obtaining various CNCs, thus broadening their applications in specific fields in the future.

Acknowledgments The authors would like to express their gratitude for financial support from the State Forestry Administration (201204803), Ministry of Science and Technology (973 project, 2010CB732204), and the Natural Science Foundation of China (No. 30930073).

References

Ago M, Endo T, Hirotsu T (2004) Crystalline transformation of native cellulose from cellulose I to cellulose II polymorph by a ball-milling method with a specific amount of water. Cellulose 11:163–167. doi:10.1023/B:CELL.0000025423.32330.fa

Araki J, Wada M, Kuga S, Okano T (2000) Birefringent glassy phase of a cellulose microcrystal suspension. Langmuir 16(6):2413–2415. doi:10.1021/la9911180

Aulin C, Ahola S, Josefsson P, Nishino T, Hirose Y, Österberg M, Wågberg L (2009) Nanoscale cellulose films with different crystallinities and mesostructures—Their surface properties and interaction with water. Langmuir 25(13):7675–7685. doi:10.1021/la900323n

Azizi Samir MAS, Alloin F, Sanchez J-Y, El Kissi N, Dufresne A (2004) Preparation of cellulose whiskers reinforced nanocomposites from an organic medium suspension. Macromolecules 37(4):1386–1393. doi:10.1021/ma030532a

Beck-Candanedo S, Roman M, Gray DG (2005) Effect of reaction conditions on the properties and behavior of wood cellulose nanocrystal suspensions. Biomacromolecules 6(2):1048–1054. doi:10.1021/bm049300p

Bondeson D, Mathew A, Oksman K (2006) Optimization of the isolation of nanocrystals from microcrystalline cellulose by acid hydrolysis. Cellulose 13(2):171–180. doi:10.1007/s10570-006-9061-4

Driemeier C, Calligaris GA (2011) Theoretical and experimental developments for accurate determination of crystallinity of cellulose I materials. J Appl Crystallogr 44(1):184–192. doi:10.1107/S0021889810043955

Elazzouzi-Hafraoui S, Nishiyama Y, Putaux J-L, Heux L, Dubreuil F, Rochas C (2007) The shape and size distribution of crystalline nanoparticles prepared by acid hydrolysis of native cellulose. Biomacromolecules 9(1):57–65. doi:10.1021/bm700769p

Esteghlalian AR, Bilodeau M, Mansfield SD, Saddler JN (2001) do enzymatic hydrolyzability and Simons' stain reflect the changes in the accessibility of lignocellulosic substrates to cellulase enzymes? Biotechnol Prog 17(6):1049–1054. doi:10.1021/bp0101177

Fan LT, Lee YH, Beardmore DR (1981) The influence of major structural features of cellulose on rate of enzymatic hydrolysis. Biotechnol Bioeng 23(2):419–424. doi:10.1002/bit.260230215

French AD, Santiago Cintrón M (2013) Cellulose polymorphy, crystallite size, and the segal crystallinity index. Cellulose 20:583–588. doi:10.1007/s10570-012-9833-y

Gao Q, Shen X, Lu X (2011) Regenerated bacterial cellulose fibers prepared by the NMMO H2O process. Carbohydr Polym 83(3):1253–1256. doi:10.1016/j.carbpol.2010.09.029

Goetz L, Mathew A, Oksman K, Gatenholm P, Ragauskas AJ (2009) A novel nanocomposite film prepared from cross-linked cellulosic whiskers. Carbohydr Polym 75(1):85–89. doi:10.1016/j.carbpol.2008.06.017

Habibi Y, Chanzy H, Vignon M (2006) TEMPO-mediated surface oxidation of cellulose whiskers. Cellulose 13(6):679–687. doi:10.1007/s10570-006-9075-y

Habibi Y, Lucia LA, Rojas OJ (2010) Cellulose nanocrystals: chemistry, self-assembly, and applications. Chem Rev 110(6):3479–3500. doi:10.1021/cr900339w

Hirota M, Tamura N, Saito T, Isogai A (2010) Water dispersion of cellulose II nanocrystals prepared by TEMPO-mediated oxidation of mercerized cellulose at pH 4.8. Cellulose 17(2):279–288. doi:10.1007/s10570-009-9381-2

Isogai T, Yanagisawa M, Isogai A (2008) Degrees of polymerization (DP) and DP distribution of dilute acid-hydrolyzed products of alkali-treated native and regenerated celluloses. Cellulose 15(6):815–823. doi:10.1007/s10570-008-9231-7

Isogai T, Yanagisawa M, Isogai A (2009) Degrees of polymerization (DP) and DP distribution of cellouronic acids prepared from alkali-treated celluloses and ball-milled native celluloses by TEMPO-mediated oxidation. Cellulose 16(1):117–127. doi:10.1007/s10570-008-9245-1

Klemm D, Kramer F, Moritz S, Lindström T, Ankerfors M, Gray D, Dorris A (2011) Nanocelluloses: a new family of nature-based materials. Angew Chem Int Ed 50(24):5438–5466. doi:10.1002/anie.201001273

Langan P, Nishiyama Y, Chanzy H (2001) X-ray structure of mercerized cellulose II at 1 Å resolution. Biomacromolecules 2:410–416. doi:10.1021/bm005612q

Liu Y, Hu H (2008) X-ray diffraction study of bamboo fibers treated with NaOH. Fiber Polym 9(6):735–739. doi:10.1007/s12221-008-0115-0

Nishiyama Y, Langan P, Chanzy H (2002) Crystal structure and hydrogen-bonding system in cellulose Iβ from synchrotron X-ray and neutron fiber diffraction. J Am Chem Soc 124(31):9074–9082. doi:10.1021/ja0257319

Revol JF, Dietrich A, Goring DAI (1987) Effect of mercerization on the crystallite size and crystallinity index in cellulose from different sources. Can J Chem 65(8):1724–1725. doi:10.1139/v87-288

Saito T, Isogai A (2004) TEMPO-mediated oxidation of native cellulose. The effect of oxidation conditions on chemical and crystal structures of the water-insoluble fractions. Biomacromolecules 5(5):1983–1989. doi:10.1021/bm0497769

Segal L, Creely JJ, Martin AE, Conrad CM (1959) An empirical method for estimating the degree of crystallinity of native cellulose using the X-Ray diffractometer. Text Res J 29(10):786–794. doi:10.1177/004051755902901003

Siqueira G, Bras J, Dufresne A (2008) Cellulose whiskers versus microfibrils: influence of the nature of the nanoparticle and its surface functionalization on the thermal and mechanical properties of nanocomposites. Biomacromolecules 10(2):425–432. doi:10.1021/bm801193d

Terech P, Chazeau L, Cavaille JY (1999) A small-angle scattering study of cellulose whiskers in aqueous suspensions. Macromolecules 32(6):1872–1875. doi:10.1021/ma9810621

van den Berg O, Schroeter M, Capadona JR, Weder C (2007) Nanocomposites based on cellulose whiskers and (semi) conducting conjugated polymers. J Mater Chem 17(26):2746–2753

Wada M, Heux L, Sugiyama J (2004) Polymorphism of cellulose I family: reinvestigation of cellulose IV. Biomacromolecules 5:1385–1391. doi:10.1021/bm0345357

Wang N, Ding E, Cheng R (2007a) Preparation and liquid crystalline properties of spherical cellulose nanocrystals. Langmuir 24(1):5–8. doi:10.1021/la702923w

Wang N, Ding E, Cheng R (2007b) Thermal degradation behaviors of spherical cellulose nanocrystals with sulfate groups. Polymer 48(12):3486–3493. doi:10.1016/j.polymer.2007.03.062

Zhang H, Wu J, Zhang J, He J (2005) 1-Allyl-3-methylimidazolium chloride room temperature ionic liquid: a new and powerful nonderivatizing solvent for cellulose. Macromolecules 38(20):8272–8277. doi:10.1021/ma0505676

Zhang J, Elder TJ, Pu Y, Ragauskas AJ (2007) Facile synthesis of spherical cellulose nanoparticles. Carbohydr Polym 69(3):607–611. doi:10.1016/j.carbpol.2007.01.019